LAWRENCE
LIVERMORE
NATIONAL
LABORATORY

LLNL-JRNL-640318

Axisymmetric curvature-driven instability in a model toroidal geometry

W. A. Farmer, D. D. Ryutov

July 3, 2013

Physics of Plasmas

Disclaimer

This document was prepared as an account of work sponsored by an agency of the United States government. Neither the United States government nor Lawrence Livermore National Security, LLC, nor any of their employees makes any warranty, expressed or implied, or assumes any legal liability or responsibility for the accuracy, completeness, or usefulness of any information, apparatus, product, or process disclosed, or represents that its use would not infringe privately owned rights. Reference herein to any specific commercial product, process, or service by trade name, trademark, manufacturer, or otherwise does not necessarily constitute or imply its endorsement, recommendation, or favoring by the United States government or Lawrence Livermore National Security, LLC. The views and opinions of authors expressed herein do not necessarily state or reflect those of the United States government or Lawrence Livermore National Security, LLC, and shall not be used for advertising or product endorsement purposes.

Axisymmetric curvature-driven instability in a model toroidal geometry

W. A. Farmer[1,2] and D. D. Ryutov[2]

[1)] *Physics and Astronomy Department, University of California Los Angeles, Los Angeles, California 90095, USA*

[2)] *Lawrence Livermore National Laboratory, 7000 East Ave., Livermore, CA 94550, USA*

(Dated: 9 July 2013)

A model problem is presented which qualitatively describes a pressure-driven instability which can occur in the divertor region of a tokamak where the poloidal field becomes small. The model problem is described by a horizontal slot with a vertical magnetic field which plays the role of the poloidal field. Line-tying boundary conditions are applied at the planes defining the slot. A toroidal field lying parallel to the planes is assumed to be very strong, thereby constraining the possible structure of the perturbations. Axisymmetric perturbations which leave the toroidal field unperturbed are analyzed. Ideal magnetohydrodynamics is used, and the instability threshold is determined by the energy principle. Because of the boundary conditions, the Euler equation is, in general, non-separable except at marginal stability. This problem may be useful in understanding the source of heat transport into the private flux region in a snowflake divertor which possesses a large region of small poloidal field, and for code benchmarking as it yields simple analytic results in an interesting geometry.

LLNL-JRNL-640318

I. INTRODUCTION

A well known feature of the flute instability is its capacity to develop even in the presence of a large confining magnetic field[1]. This instability has been studied in a number of papers; for reviews see, e.g.,[2,3]. What we consider here is a peculiar, analytically solvable configuration in which an axisymmetric plasma is confined by a combination of a very strong toroidal magnetic field and a weak poloidal magnetic field. The geometry of our model is shown in Fig. 1. The horizontal axis is the radial distance from the major axis of the device, and the vertical axis lies along the major axis, represented by the dashed-dotted line, which is defined to be the z direction. The plasma is shown as the gray shaded region. The magnetic field is $\mathbf{B} = B_t\hat{\phi} + B_p\hat{\mathbf{z}}$ with $\hat{\phi}$ pointing into the page. On the figure, the toroidal field, B_t, is into the page and indicated by the blue 'x'es, and the poloidal field, B_p, is vertical and indicated by the red lines. In the vertical direction, the plasma is limited by conducting plates, illustrated by the green lines. In the presence of a vertical field, the line-tying boundary conditions can stabilize the plasma[3].

The plasma pressure, p, is assumed to be very small compared to the toroidal field magnetic pressure so that, $\beta_t \equiv 8\pi p/B_t^2 \ll 1$ (here and throughout the paper, we use the CGS system of units). On the other hand, the poloidal field, B_p, can be arbitrary, i.e. the parameter, $\beta_p \equiv 8\pi p/B_p^2$ can vary from zero to infinity. The case of a very small B_p (and large β_p) is of relevance to the plasma stability near the null of the poloidal field in the divertor; we focus our analysis on just this case, $\beta_p \gg 1$. We later establish a qualitative correspondence between our simple model and a divertor geometry.

We consider a uniform B_p; the equilibrium is provided by the interaction of the poloidal current with density, j_p, with the toroidal field,

$$\frac{\mathrm{d}p}{\mathrm{d}r} = -j_p B_t/c, \tag{1}$$

where c is the speed of light. From Ampère's law, the current density can be eliminated leading to the equation

$$\frac{\mathrm{d}}{\mathrm{d}r}\left(p + \frac{B_t^2}{8\pi}\right) + \frac{B_t^2}{4\pi r} = 0. \tag{2}$$

Solving for the field in terms of the pressure gives the result that

$$B_t^2(r) = \left(\frac{r_0}{r}\right)^2 B_{t0}^2 - 8\pi \int_{r_0}^{r} \frac{\mathrm{d}p(r')}{\mathrm{d}r'} \left(\frac{r'}{r}\right)^2 \mathrm{d}r', \tag{3}$$

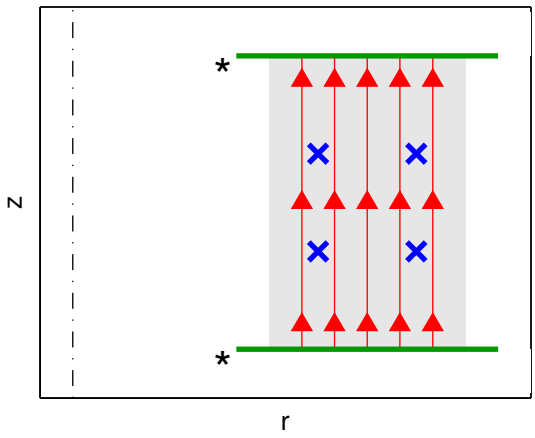

FIG. 1. Magnetic geometry of problem of interest. Vertical axis is major axis, indicated by the dash-dotted line, and the horizontal axis is radial distance from the major axis. Shaded, gray region is an annulus of plasma. Blue 'x'es represent the toroidal field that points into the page. Poloidal field is represented by the red lines. Conducting plates are represented by the thick green lines. Possibly stable or unstable depending on value of β_p and distance between plates. Asterisks are used to make connection to Fig. 2.

where B_{t0} is a constant which characterizes the vacuum fields that would exist in the absence of a plasma, and r_0 is a characteristic radius used to specify the toroidal field. Because $\beta_t \ll 1$, the second term in Eq. (3) is negligible with the toroidal field well described by the vacuum field alone. In Appendix A, we discuss a more general equilibrium where the toroidal current is allowed and B_p can have a radial dependence.

If the poloidal field vanishes, the plasma is obviously unstable with respect to the toroidally-symmetric ($n = 0$) flute mode. Plasma convection in the form of toroidally-symmetric "rolls" would then ensue. Inclusion of a poloidal field anchored to the conducting plates will provide some stabilizing effect due to the bending of the field lines. Eventually, at strong enough poloidal field, the plasma is stabilized. Our paper contains a derivation of the stability limit of this peculiar flute-like $n = 0$ mode, which does not perturb the strong toroidal field but does perturb a weak poloidal field. Somewhat surprisingly, the stabilization occurs at relatively low values of B_p, corresponding to $\beta_p \gg 1$ when parameters for a generic tokamak are used.

Beyond the application to divertor physics, the problem posed here is simple enough to

yield analytic results, but nevertheless, possesses an interesting geometry. The results could be useful for code benchmarking. Further, the conclusions help to elucidate interesting basic physics.

This manuscript is organized as follows. The simplified geometry and its relation to the snowflake divertor is discussed in Section II. A general theoretical framework is then described in Section III. The governing equations and boundary conditions are stated with the energy principle[4] which properly accounts for the small parameters present in the problem, and an Euler equation is then given for the axisymmetric perturbations of interest. Instability thresholds are then derived in Section IV. Discussion and major conclusions are presented in Section V. Finally, a more general equilibrium is discussed in Appendix A, and separability in an infinite plasma is discussed in Appendix B.

II. RELATION TO DIVERTOR

This problem is a simple model of the divertor region in a tokamak with the divertor plates enforcing line-tying boundary conditions. The magnetic geometry in a real divertor is, of course, more complex, but many of the fundamental features are contained by the simple problem described above. Since the toroidal beta, $\beta_t = 8\pi p/B_t^2$, is much smaller than unity, the toroidal field acts as an additional constraint on the system, making it energetically unfavorable to perturb the toroidal field. The poloidal field, in contrast, vanishes at the null point, creating a region in the plasma over which the poloidal beta, $\beta_p = 8\pi p/B_p^2$, is much greater than unity. An axisymmetric, quasi-flute mode can then be considered which leaves the toroidal field completely unperturbed, but allows for perturbations in the poloidal field. Because the mode leaves the toroidal field unperturbed, this mode is axisymmetric (i.e. it does not depend on the toroidal coordinate), and the toroidal field strength is irrelevant to both the growth rates and the instability thresholds. These qualities reflect the quasi-flute nature of the instability with the line-tying boundary conditions stabilizing the mode to a degree in the presence of the poloidal field.

For a standard divertor configuration, the region over which $\beta_p = 8\pi p/B_p^2 \gg 1$ is generally quite small. In contrast, in a snowflake divertor[5,6], this region is much larger because the null is second order as opposed to the first order null in the standard divertor. As a result, the poloidal field scales as $B_p \propto d^2$ where d is the distance from the null point. For a

given value of β_p in the midplane, the region over which β_p exceeds some characteristic value is dramatically larger in the snowflake divertor than in a standard divertor as is shown in previous papers[7,8] and in Section V. Experimentally, the snowflake divertor has been realized on NSTX[9,10], TCV[11–13], and DIII-D[14]. The resulting plasmas had many favorable qualities, one of which was spreading of the heat flux to the private flux region and splitting it over multiple strike points. In the vicinity of the null, sharp pressure gradients exist which, when combined with the curvature of the toroidal field, can drive convective processes[7,8]. The axisymmetric, quasi-flute mode is one possible source of this convection.

The geometry of the flux surfaces present in a snowflake divertor is shown in Fig. 2. The horizontal axis is the radial coordinate and is expressed in terms of x where $r = R + x$, R being the major radius of the $B_p = 0$ circle and r, the radial distance from the major axis. The vertical axis, z, runs parallel to the major axis, and the toroidal coordinate lies into the page. The black and red lines represent the nested magnetic flux surfaces with the thicker black lines representing the separatrices. The thick green lines are representative of the divertor plates upon which heat is deposited due to the streaming of the plasma along the field lines. The core plasma is contained in the upper most sextant with the two adjacent sextants containing the scrape off layer (SOL). The three remaining sextants in the lower half plane are private flux regions and are largely isolated from the remainder of the plasma. In modeling the private flux region, there exist large pressure gradients normal to the flux surfaces. These pressure gradients combined with regions of unfavorable curvature may give rise to plasma instability which leads to heat transport across flux surfaces. This can lead to heat flux being deposited upon the lower two divertor plates, thus spreading the incident energy from two strike points to four.

The complicated geometry present in the snowflake, while certainly important, is not included in our zeroth order examination of stability. To make the connection between the general divertor geometry and the simplified geometry, two divertor plates have been marked by an asterisk in both Fig. 1 and Fig. 2. Focus is given to the private flux region in Fig. 2 that has red lines with the other private flux regions ignored. If the orientations of the two plates in Fig. 2 are changed such that they are parallel to each other and the connecting flux surfaces are rectified, Fig. 2 is transformed into Fig. 1 with the asterisks marking the position to which the plates have shifted. In making the transformation, the orientation of the coordinates is chosen such that the vector $\hat{\mathbf{z}}$ points in the vertical direction, the vector $\hat{\mathbf{r}}$

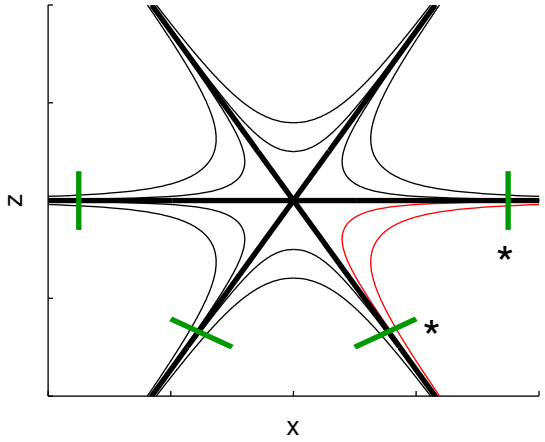

FIG. 2. Flux surfaces of snowflake divertor. Horizontal axis is radial distance from the null point. Green lines represent divertor plates, thicker black lines are separatrices, and thin lines are plasma flux surfaces. If red lines are stretched vertically and divertor plates marked by asterisks are reoriented, geometry reduces to Fig. 1 which is possibly unstable.

points to the right, and the toroidal direction, $\hat{\phi}$, points into the board. The divertor plates exist as planes located at $z = 0,\ L$, at which the appropriate boundary conditions must be imposed.

III. THEORY

In performing stability analysis, the ideal MHD energy principle[4] is employed in the form

$$\omega^2 = \frac{W_F}{K}, \tag{4}$$

$$K = \frac{1}{2}\int \rho\,|\xi|^2\ \mathrm{d}V, \tag{5}$$

$$W_F = \frac{1}{2}\int \left[\gamma p\,(\nabla\cdot\xi)^2 + (\nabla\cdot\xi)\,(\xi\cdot\nabla p) - \frac{\mathbf{j}}{c}\cdot(\mathbf{Q}\times\xi) + \frac{Q^2}{4\pi}\right]\ \mathrm{d}V, \tag{6}$$

In the above expressions, ξ represents the plasma displacement from equilibrium and is assumed to have harmonic time dependence with frequency ω. The kinetic energy is equal to $-\omega^2 K$, and the potential energy is comprised solely of a fluid term, W_F. The mass density is defined by ρ, γ is the ratio of specific heats, p is the pressure, $\mathbf{j}$ is the equilibrium current density, $\mathbf{Q} = \nabla\times(\xi\times\mathbf{B})$ is the perturbed magnetic field, and $\mathbf{B}$ is the equilibrium magnetic field. Because the plates are assumed to be rigid, ξ_z must vanish at the plates. Further, the

divertor plates are assumed to be perfectly conducting so that line-tying boundary conditions can be assumed. The fact that the equilibrium magnetic field has a normal component at the plates should not be viewed as a contradiction of these boundary conditions. The equilibrium component of the magnetic field is assumed to have penetrated into the divertor plates on a time scale much longer than that which characterizes the unstable modes. From Ohms' law for a perfectly conducting plasma,

$$\mathbf{E} = \frac{i\omega}{c}\xi \times \mathbf{B}. \tag{7}$$

In order that the tangential components of the electric field vanish at the plates, the other two components of the plasma displacement, ξ_r and ξ_ϕ, must also vanish. These boundary conditions justify the neglect of the boundary terms in the energy principle. At marginal stability, the potential energy will satisfy the relation $W_F = 0$.

Perturbations are considered which are of the form,

$$\xi \times B_t\hat{\phi} = \nabla\psi. \tag{8}$$

With the above choice, ξ_ϕ is not related to ψ and is left as a free parameter. However, in the situation considered, the plasma motion in the ϕ direction decouples from the motion in the poloidal plane and represents a stable, torque mode. For this reason, $\xi_\phi = 0$ is chosen. With this choice and the above relation, the toroidal field remains unperturbed. This is necessary because the toroidal field is very strong. Because the toroidal field is unperturbed, the instability threshold is independent of B_t. Further, we specialize to modes that are axisymmetric. From the above expression, it is clear that ψ cannot depend on ϕ, and with the choice that $\xi_\phi = 0$, the convection will take place only in the poloidal plane. This choice of perturbations automatically excludes other possible unstable modes, leading the final instability threshold to be a sufficient but not necessary condition. Substituting Eq. (8) into Ohm's law, we obtain

$$\mathbf{E} = \frac{i\omega}{c}\left[\nabla\psi + \xi \times \mathbf{B}_p\right]. \tag{9}$$

Because axisymmetric displacements are considered and $\xi_\phi = 0$ is chosen, the two terms in Eq. (9) are orthogonal. From these conclusions, the physical interpretation of ψ becomes clear: it is proportional to that portion of the electrostatic potential that gives rise to electric fields perpendicular to the toroidal field. The boundary conditions can then be summarized

as

$$\xi_r|_{z=0,\,L} = 0, \quad \xi_z|_{z=0,\,L} = 0, \tag{10}$$

$$\left.\frac{\partial\psi}{\partial r}\right|_{z=0,L} = 0, \quad \left.\frac{\partial\psi}{\partial z}\right|_{z=0,L} = 0. \tag{11}$$

From Eq. (8), the potential energy can be computed. To do so, the perturbed magnetic field and the divergence of the plasma displacement are computed using the assumption that the toroidal field is well approximated by its vacuum field which scales as $1/r$. These quantities are then expressed as

$$\nabla\cdot\xi = \frac{2}{rB_t}\frac{\partial\psi}{\partial z} = \frac{2}{r}\xi_r, \tag{12}$$

$$\mathbf{Q} = \hat{\mathbf{r}}\frac{B_p}{B_t}\frac{\partial^2\psi}{\partial z^2} - \hat{\mathbf{z}}\frac{1}{r}\frac{\partial}{\partial r}\left(\frac{rB_p}{B_t}\frac{\partial\psi}{\partial z}\right) = \hat{\mathbf{r}}B_p\frac{\partial\xi_r}{\partial z} - \hat{\mathbf{z}}\frac{1}{r}\frac{\partial}{\partial r}\left(rB_p\xi_r\right). \tag{13}$$

These expressions are then combined with the expression for the equilibrium current distribution

$$\frac{4\pi\mathbf{j}}{c} = \hat{\mathbf{z}}\frac{1}{r}\frac{\mathrm{d}}{\mathrm{d}r}\left(rB_t\right), \tag{14}$$

where it has been assumed that B_p is constant. Substituting the previous relations into the energy principle gives rise to the following equation for the potential energy,

$$W_F = \int\left[\frac{2\gamma p\xi_r^2}{r^2} + \frac{\xi_r^2}{r}\frac{\mathrm{d}p}{\mathrm{d}r} + \frac{B_p^2}{8\pi}\left(\left(\frac{\partial\xi_r}{\partial z}\right)^2 + \left(\frac{1}{r}\frac{\partial(r\xi_r)}{\partial r}\right)^2\right)\right]\mathrm{d}V. \tag{15}$$

The boundary condition that $\xi_z = 0$ at the divertor plates and the relation in Eq. (12) coupled with integration by parts have been used to obtain the form shown in Eq. (15). At this point, further simplification can be made if it is assumed that the perturbations are localized at a radius much larger than any other scale length in the problem. This is valid because the pressure variation in the divertor region is very rapid compared to R. This assumption allows the first term in Eq. (15) to be neglected in favor of the second term and to expand derivatives in r using the relation $r = R + x$ to lowest order in $1/R$. If this is done, Eq. (15) becomes

$$W_F = \int\left[\frac{\xi_r^2}{R}\frac{\mathrm{d}p}{\mathrm{d}x} + \frac{B_p^2}{8\pi}\left(\left(\frac{\partial\xi_r}{\partial z}\right)^2 + \left(\frac{\partial\xi_r}{\partial x}\right)^2\right)\right]\mathrm{d}V. \tag{16}$$

The first term in the above equation is the source of free energy which drives the instability.

Next, it is useful to derive the resulting Euler equation associated with the energy principle. This can be done either from the energy principle or directly from the equations of

motion from which the energy principle is derived. Either way, the same equation results, and it is more easily expressed in terms of the function, ψ, than in terms of ξ_r. The resulting differential equation is

$$\nabla \cdot \left[\frac{\rho\omega^2}{2} \nabla\psi \right] + \frac{\partial^2}{\partial z^2} \left[-\frac{1}{R} \frac{\mathrm{d}p}{\mathrm{d}x} \psi + \frac{B_p^2}{8\pi} \nabla^2 \psi \right] = 0, \tag{17}$$

where $\nabla = \hat{\mathbf{x}}\partial/\partial x + \hat{\mathbf{z}}\partial/\partial z$. The above equation is inseparable in general, i.e. the solution cannot be written as a product of a function of x and a function of z. This makes it difficult to obtain the normal modes when not at marginal stability. Semi-analytic methods exist to solve non-separable problems[15], however, since this is a model problem, a sophisticated treatment is postponed until a more realistic analysis of the precise geometry can be performed. The problem is separable if the conducting plates are removed and the plasma is assumed to be of infinite extent. This case is examined in Appendix B.

IV. INSTABILITY THRESHOLDS

To obtain an instability threshold, a Gaussian pressure gradient is first assumed,

$$\frac{\mathrm{d}p}{\mathrm{d}x} = -\frac{p_0}{\sqrt{\pi}\delta} e^{-\frac{x^2}{\delta^2}}, \tag{18}$$

where p_0 and δ are constants used to specify the amplitude and width of the pressure gradient. The pressure gradient is steepest at $x = 0$ or $r = R$. Further, the pressure profile is assumed to vanish as $x \to \infty$ so that p_0 can be taken to be the total plasma pressure. This profile describes the outer edge of the plasma. The inner edge is neglected, and it is assumed to be well separated from the radially localized trial function. A trial function which satisfies the boundary conditions is chosen to be

$$\psi = \psi_0 \left(1 - \cos kz\right) \frac{1}{\left(\sqrt{\pi} l\right)^{1/2}} e^{-\frac{(x-x_0)^2}{2l^2}}, \tag{19}$$

$$\xi_r = \frac{\psi_0}{B_t} k \sin kz \frac{1}{\left(\sqrt{\pi} l\right)^{1/2}} e^{-\frac{(x-x_0)^2}{2l^2}}, \tag{20}$$

$$\xi_z = \frac{\psi_0}{B_t} \left(1 - \cos kz\right) \frac{x - x_0}{l^2} \frac{1}{\left(\sqrt{\pi} l\right)^{1/2}} e^{-\frac{(x-x_0)^2}{2l^2}}. \tag{21}$$

The toroidal field, B_t, in the above expressions is evaluated at the major radius, R, and is taken to be a constant. The wave number, k, is chosen to be $k = 2\pi/L$ where, as before, L is the distance between the two divertor plates. The quantity, x_0, describes the position

at which the trial function, ψ, is localized and may not coincide with the point at which the pressure gradient is steepest. The quantity, l, describes the spatial width over which the trial function is localized. To be consistent with the assumptions made thus far, it is assumed that $R \gg L$, l.

If the trial function is substituted into Eqs. (5) and (16), and it is assumed that the plasma density does not vary with radial position, the integrations can be easily performed. To do so, the differential volume element is taken to be $\mathrm{d}V = \mathrm{d}x\,\mathrm{d}z R\,\mathrm{d}\phi$. Integration over x is performed with the limits of the integral expanded to the interval, $(-\infty, \infty)$, due to the rapid convergence of the integrand. After performing all integrations, the energy principle results in

$$\omega^2 = \frac{B_p^2 k^2}{8\pi\rho} \frac{\left(-\frac{8\pi p_0}{B_p^2} \frac{e^{-\frac{x_0^2}{l^2+\delta^2}}}{\sqrt{\pi(l^2+\delta^2)}} \frac{L^2}{R} + k^2 L^2 + \frac{L^2}{2l^2} \right)}{\frac{1}{2}k^2 L^2 + \frac{3L^2}{4l^2}}, \tag{22}$$

which leads to the sufficient condition for instability,

$$\beta_p > R\left(k^2 + \frac{1}{2l^2}\right)\sqrt{\pi(l^2+\delta^2)}e^{\frac{x_0^2}{l^2+\delta^2}}. \tag{23}$$

It is not surprising that $x_0 = 0$ gives the smallest limit, and this choice is made. Next, the instability threshold can be further minimized by choosing

$$l^2 = \frac{1}{4k^2}\left[1 + \sqrt{1 + 16k^2\delta^2}\right]. \tag{24}$$

Thus, minimizing Eq. (23) leads to

$$\beta_p > \frac{kR}{2}\left[1 + \frac{2}{1+\sqrt{1+16k^2\delta^2}}\right]\sqrt{\pi\left(1 + \sqrt{1+16k^2\delta^2} + 4k^2\delta^2\right)}. \tag{25}$$

The right hand side of this equation is a monotonically increasing function of $k^2\delta^2$ suggesting that the smallest instability threshold will occur when $k\delta \ll 1$. In this limit,

$$\beta_p > \sqrt{2\pi}kR. \tag{26}$$

This limit requires that $L \gg \delta$, a condition which is easily satisfied in the divertor.

The lowest threshold for instability occurs when the pressure drop is rapid and the gaussian pressure gradient approaches a delta-function. This suggests that the Euler equation be examined more closely for a delta-function pressure gradient. As will be shown below, when

this choice is made, Eq. (17) is separable at marginal stability and can be solved exactly. Thus, the pressure gradient is

$$-\frac{\mathrm{d}p}{\mathrm{d}x} = p_0\delta(x). \tag{27}$$

The problem is reduced to solving the equation

$$\frac{\partial^2}{\partial z^2}\left[\frac{p_0}{R}\delta(x)\psi + \frac{B_p^2}{8\pi}\nabla^2\psi\right] = 0, \tag{28}$$

subject to the boundary conditions in Eq. (11). The delta-function gives a jump condition for ψ which must be satisfied by connecting the two solutions on either side of the discontinuity. Away from the gradient, the equation reduces to Laplace's equation for the second order derivative of ψ with respect to z. The solutions are easily written as

$$\frac{\partial^2\psi}{\partial z^2} = -k^2 f_1(x)\cos(kz) - k^2 f_2(x)\sin(kz), \tag{29}$$

$$\frac{\partial\psi}{\partial z} = -k f_1(x)\sin(kz) + k f_2(x)\cos(kz) + k f_3(x), \tag{30}$$

$$\psi = f_1(x)\cos(kz) + f_2(x)\sin(kz) + f_3(x)kz + f_4(x). \tag{31}$$

Applying the boundary conditions leads to the solution

$$\psi = f(x)\left[(kL - \sin kL)(1 - \cos kz) - (1 - \cos kL)(kz - \sin kz)\right], \tag{32}$$

where k is determined by the condition that $\partial\psi/\partial z$ must vanish at $z = L$. This gives two different quantization conditions for k which depend on whether ψ is even or odd about $z = L/2$. The quantization conditions for k are

$$\sin\frac{kL}{2} = 0 \quad \text{(even)}, \tag{33}$$

$$\tan\frac{kL}{2} = \frac{kL}{2} \quad \text{(odd)}. \tag{34}$$

The most restrictive condition is given by the longest wavelength. For the even mode, the longest wavelength solution is $kL = 2\pi$, and for the odd mode, $kL = 2.86\,\pi$. Thus, the most restrictive instability threshold is given by an even mode, and $kL = 2\pi$ will be assumed in the analysis that follows. Further, from the differential equation, the function, $f(x)$, can be determined so that the form of ψ at marginal stability is

$$\psi = \psi_0 e^{-k|x|}\left(1 - \cos kz\right). \tag{35}$$

Finally, the jump condition is determined by integrating Eq. (28) on the interval $(-\epsilon, \epsilon)$ and taking the limit as $\epsilon \to 0$. This gives the condition that

$$\frac{p_0}{R}\left.\frac{\partial^2 \psi}{\partial z^2}\right|_{x=0} + \Delta\left(\frac{B_p^2}{8\pi}\frac{\partial^3 \psi}{\partial z^2 \partial x}\right) = 0, \tag{36}$$

where Δ denotes the difference in the limit of the function as $x = 0$ is approached from both the right and the left. Substituting in the form of ψ results in

$$\frac{8\pi p_0}{B_{p0}^2} > 2kR, \tag{37}$$

where the inequality is added at this point as a sufficient condition for instability. It is clear at this point that if $L \to \infty$, $k \to 0$, and the plasma is inherently unstable, as is expected.

From ψ, the functions ξ_r and ξ_z can be computed and are

$$\xi_r = \frac{k}{B_t}\psi_0 e^{-k|x|}\sin kz, \tag{38}$$

$$\xi_z = -\frac{\mathrm{sgn}(x)k}{B_t}\psi_0 e^{-k|x|}\left(1 - \cos kz\right), \tag{39}$$

where

$$\mathrm{sgn}(x) = \frac{x}{|x|}. \tag{40}$$

The discontinuity in ξ_z at $x = 0$ is characteristic of the Rayleigh-Taylor instability. Figure 3 shows the displacement that occurs in the linear stage of the instability. The black dashed lines represent equilibrium plasma surfaces, and the solid blue lines show how the plasma is displaced as the instability grows. The conducting planes are placed at $z = 0$ and $z = L$. The instability decays away from the pressure gradient in the x-direction as can be seen in the figure. It is obvious from this picture that this instability will lead to convective mixing of the plasma and increased transport across field lines.

A meaningful comparison can now be made between the two instability thresholds in Eqs. (26) and (37). Equation (26) was the limiting form of Eq. (25) when the Gaussian profile becomes a delta-function. While Eq. (25) is more general than Eq. (37), Eq. (37) gives a lower instability threshold than Eq. (26). This is not surprising as the actual eigenfunction was obtained in deriving Eq. (37) instead of using a trial function. However, the trial function method is useful when considering more general pressure profiles.

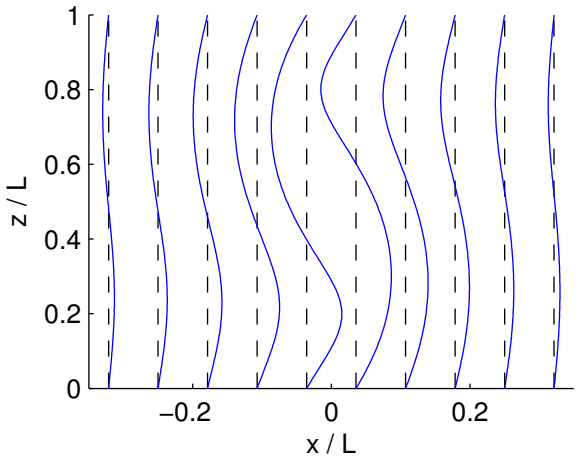

FIG. 3. Perturbed plasma surfaces of most unstable mode at marginal stability. Vertical axis is z-coordinate scaled to distance between plates, L. Horizontal axis is distance from peek in pressure gradient scaled to distance between plates. Dashed black lines are the equilibrium plasma position, and solid blue lines are the perturbed plasma displacement as given in Eqs. (38) and (39). Mode drives poloidal convection and would lead to transport of heat flux.

V. CONCLUSIONS

Using the instability limit shown in Eq. (37), an order of magnitude estimate can now be made for a generic tokamak. The smallest k value is substituted into the equation resulting in the expression

$$\beta_p > 4\pi \frac{R}{L}, \tag{41}$$

where R/L is a parameter greater than unity. For a standard tokamak, $R/L \approx 5$ is reasonable, resulting in the sufficient condition for instability,

$$\beta_p \gtrsim 60. \tag{42}$$

For an ELM event, it is typical that $\beta_p \sim 10^{-2}$ in the midplane with β_p decreasing by a factor of 20-30 during normal operation[18,19]. If a snowflake divertor is assumed, then during an ELM event, the instability condition would be satisfied for distances, d, from the null point, satisfying $d < a/9$, where a is the minor radius. For an ITER-scale facility, this means that $d < 20\,\text{cm}$ would correspond to a region over which this quasi-flute mode could reasonably occur, and convection would result. Normal operation causes the region over which convection occurs to decrease roughly by a factor of two. If a standard divertor is

assumed, due to the smaller flux expansion, the convection region is much smaller, shrinking to $d < a/67$ during an ELM event. Thus, this mode would not significantly contribute to convection in a standard divertor configuration. For a spherical tokamak, this convection region is larger as the smaller aspect ratio of the tokamak means that a value of $R/L \approx 2$ would be more appropriate. In the presence of a snowflake divertor,

$$\beta_p \gtrsim 24, \tag{43}$$

results, and convection would occur over a larger region satisfying $d < a/7$ during an ELM event. These results may help guide the further investigation of convection in the snowflake divertor.

It must be emphasized that these results are sufficient conditions for instability, but are by no means necessary. The type of mode considered in this manuscript is a special class of instabilities, but they are not general. Ballooning modes are another possible source of instability, e.g.[2,3]. For these modes, the large distance traversed by the magnetic field line between the two conducting plates allows for slow variations of the perturbation along the field line with rapid variations across the field line. This instability will necessarily perturb the toroidal field. However, this effect will be offset by the large distance traversed by the field line between the two plates. As a result, these two competing effects can result in instability, but in contrast to the axisymmetric, quasi-flute mode, the growth rates and instability threshold will necessarily depend on the toroidal field strength. The analysis of these ballooning modes for the problem posed in this manuscript is postponed to a later publication, but it is important to remember that the mode examined in this manuscript is not the only possible source of convection.

One more connection of our analysis is that with the gravitational instability. Previous work has been done in examining convection in a plasma in the presence of a horizontal magnetic field and a vertical gravitational force in order to model the Rayleigh-Taylor instability for a magnetized fluid. Newcomb[16] presented a calculation in which he showed that the Schwarzschild criterion for convection in a compressible, ideal fluid holds even for an electrically conducting fluid in the presence of a horizontal magnetic field. The irrelevance of the strength of the magnetic field to the convection criterion reflects the fact that flute modes are driving the convection. The gravitational force in their problem plays the role of the toroidal curvature pressure term that appears in the analysis presented here. Zweibel

and Bruhwiler[17] extended these ideas by performing the calculation within a vertical slot with line-tying boundary conditions enforced at the two planes. Their work most closely resembles the work presented here. The difference is that they consider a situation where there is no component of the magnetic field parallel to the plates, only the normal component. With the inclusion of a strong horizontal field oriented parallel to the plates, a correspondence can be shown between their work and this paper. The presence of a strong guide field serves to make the plasma incompressible, leading to stronger plasma stability.

In summary, we have derived instability thresholds for β_p for an axisymmetric, curvature-driven instability in a model, toroidal geometry. Conducting plates are shown to limit the smallest possible axial wavenumber. These limits hold even as the toroidal field becomes arbitrarily large. These results have been applied to a divertor, and it has been shown that the convection region is significantly larger in a snowflake divertor than in a normal divertor configuration, and this result could explain the increased convection observed in experiments[12,13].

ACKNOWLEDGMENTS

This work performed under the auspices of the U.S. Department of Energy by Lawrence Livermore National Laboratory under Contract DE-AC52-07NA27344.

Appendix A: General Equilibrium

If a toroidal current density, j_t is allowed, the equilibrium is now defined by

$$\frac{\mathrm{d}p}{\mathrm{d}r} = \frac{j_t B_p}{c} - \frac{j_p B_t}{c}. \tag{A1}$$

This allows the pressure to be partitioned into two functions, p_p and p_t, satisfying $\mathrm{d}p_p/\,\mathrm{d}r = j_t B_p/c$ and $\mathrm{d}p_t/\,\mathrm{d}r = -j_p B_t/c$. Using Ampère's law and solving for the fields leads to

$$B_p^2(r) = B_{p0}^2 - 8\pi p_p(r), \tag{A2}$$

$$B_t^2(r) = B_{t0}^2 \left(\frac{r_0}{r}\right)^2 - 8\pi \int_{r_0}^{r} \frac{\mathrm{d}p_t}{\mathrm{d}r'} \left(\frac{r'}{r}\right)^2 \mathrm{d}r', \tag{A3}$$

where now, the poloidal field can vary.

Allowing the poloidal field to vary causes p_t to replace p in Eqs. (15) and (16), and the Euler equation is now given by

$$\nabla \cdot \left[\frac{\rho\omega^2}{2}\nabla\psi\right] + \frac{\partial^2}{\partial z^2}\left[-\frac{1}{R}\frac{\mathrm{d}p_t}{\mathrm{d}x}\psi + \frac{B_p^2}{8\pi}\nabla^2\psi + \frac{\mathrm{d}}{\mathrm{d}x}\left(\frac{B_p^2}{8\pi}\right)\frac{\partial\psi}{\partial x}\right] = 0, \tag{A4}$$

In considering a delta-function pressure gradient, the poloidal field can now vary giving

$$\frac{\mathrm{d}p_t}{\mathrm{d}x} = -p_{t0}\delta(x), \tag{A5}$$

$$B_p = \begin{cases} B_{pi}, & x < 0 \\ B_{p0}, & x > 0 \end{cases}. \tag{A6}$$

Equation (36) is altered only by replacing p_0 with p_{t0}, and the values of B_p on both sides of the discontinuity must be accounted for when computing the jump condition. This leads to the instability threshold

$$\frac{8\pi p_{t0}}{B_{p0}^2} > kR\left(1 + \frac{B_{pi}^2}{B_{p0}^2}\right). \tag{A7}$$

If $B_{pi} = B_{p0}$, then $p_{t0} = p_0$ and this reduces to the previous result. If the poloidal field is confining as much of the plasma pressure as it possibly can, $B_{pi}/B_{p0} \ll 1$ and $8\pi p_p/B_{p0}^2 = 1$. If this is the case, the instability limit becomes

$$\frac{8\pi p_0}{B_{p0}^2} > kR + 1 \approx kR, \tag{A8}$$

decreasing the instability threshold by a factor of two. Again, taking $R/L \approx 5$, then for an ELM event in a snowflake divertor, $d < a/7$, a modest improvement. For ITER, this is satisfied for distances $d < 29$ cm from the null, which again reduces by a factor of two for steady state operation.

Appendix B: Infinite Medium

If an infinite medium is considered, Eq. (17) is separable. The function, ψ, can now be decomposed in terms of Fourier harmonics in the z direction so that $\psi \propto \exp(ikz)$. Allowing for a poloidal field that varies in the x direction (see Appendix A), the Euler equation becomes

$$\frac{\partial}{\partial x}\left[\left(\frac{\rho\omega^2}{2k^2} - \frac{B_p^2}{8\pi}\right)\frac{\partial\psi}{\partial x}\right] + \left[\frac{1}{R}\frac{\mathrm{d}p_t}{\mathrm{d}x} - k^2\left(\frac{\rho\omega^2}{2k^2} - \frac{B_p^2}{8\pi}\right)\right]\psi = 0. \tag{B1}$$

If a delta function pressure profile is assumed, and the plasma density is assumed to be a step-function, then the equation is solvable with

$$\psi = \psi_0 e^{ikz-k|x|}. \tag{B2}$$

The jump condition caused by the delta-function gives the dispersion relation

$$\frac{\omega^2}{k^2} = \frac{B_{p0}^2}{4\pi\bar{\rho}}\frac{1}{kR}\left[-\frac{8\pi p_{t0}}{B_{p0}^2} + kR\left(1+\frac{B_{pi}^2}{B_{p0}^2}\right)\right], \tag{B3}$$

where the same notations in Appendix A have been used, and $\bar{\rho}$ is the average plasma density across the jump. It is noteworthy that the instability threshold from the above expression is the same as given in Appendix A reflecting the separability of both cases. However, since the plasma is infinite, k can take on arbitrarily small values, and the plasma will be unstable for any pressure jump, whatsoever.

REFERENCES

[1]M. M. Rosenbluth and C. L. Longmire, Ann. Phys. **1**, 120 (1957).

[2]J. P. Freidberg, *Ideal Magnetohydrodynamics* (Plenum, New York, 1987).

[3]B. B. Kadomtsev, *Hydromagnetic Stability of a Plasma*, in Reviews of Plasma Physics, Vol. 2, edited by M. A. Leontovich (Consultants Bureau, New York, 1966).

[4]I. B. Bernstein, E. A. Frieman, M. D. Kruskal, and R. M. Kulsrud, Proc. Roy. Soc. A **244**, 17 (1958).

[5]D. D. Ryutov, Phys. Plasmas **14**, 064502 (2007).

[6]D. D. Ryutov, M. A. Makowski, and M. V. Umansky, Plasma Phys. Control. Fusion **52** 105001 (2010).

[7]D, D, Ryutov, R. H. Cohen, T. D. Rognlien, and M. V. Umansky, Contrib. Plasma Phys. **52**, 539 (2012).

[8]D. D. Ryutov, R. H. Cohen, T. D. Rognlien, and M. V. Umansky, Plasma Phys. Control. Fusion **54**, 124050 (2012).

[9]V. A. Soukhanovskii, R. E. Bell, A. Diallo, S. Gerhardt, S. Kaye, E. Kolemen, B. P. Leblanc, A. G. McLean, J. E. Menard, S. F. Paul, M. Podesta, R. Raman, T. D. Rognlien, A. L. Roquemore, D. D. Ryutov, F. Scotti, M. V. Umansky, D. Battaglia, M. G. Bell, D. A. Gates, R. Kaita, R. Maingi, D. Mueller, and S. A. Sabbagh, Phys. Plasmas **19**, 082504 (2012).

[10]V. A. Soukhanovskii, J.-W. Ahn, R. E. Bell, D. A. Gates, S. Gerhardt, R. Kaita, E. Kolemen, B. P. LeBlanc, R. Maingi, M. Makowski, R. Maqueda, A. G. McLean, J. E. Menard, D. Mueller, S. F. Paul, R. Raman, A. L. Roquemore, D. D. Ryutov, S. A. Sabbagh, and H. A. Scott, Nucl. Fusion **51**, 012001 (2011).

[11]F. Piras, S. Coda, I. Furno, J.-M. Moret, R. A. Pitts, O. Sauter, B. Tal, G. Turri, A. Bencze, B. P. Duval, F. Felici, A. Pochelon, and C. Zucca, Plasma Phys. Control. Fusion **51**, 055009 (2009)

[12]F. Piras, S. Coda, B. P. Duval, B. Labit, J. Marki, S. Yu Medvedev, J.-M. Moret, A. Pitzschke, and O. Sauter, Plasma Phys. Control. Fusion **52**, 124010 (2010).

[13]F. Piras, S. Coda, B. P. Duval, B. Labit, J. Marki, S. Yu. Medvedev, J.-M. Moret, A. Pitzshke, and O. Sauter, Phys. Rev. Lett. **105**, 155003 (2010).

[14]S. L. Allen, in *24th IAEA Fusion Energy Conference*, San Diego, USA, 2012, p. 623.

[15]E. G. Evstatiev, G. L. Delzanno, and J. M. Finn, Phys. Plasmas, **13**, 072902 (2006).

[16]W. A. Newcomb, Phys. Fluids **4**, 391 (1961).

[17]E. G. Zweibel and D. L. Bruhwiler, Astrophys. J. **399**, 318 (1992).

[18]A. Loarte, G. Saibene, R. Sartori, D. Campbell, M. Becoulet, L. Horton, T. Eich, A. Herrmann, G. Matthews, N. Asakura, A. Chankin, A. Leonard, G. Porter, G. Gederici, G. Janeschitz, M. Shimada, and M. Sugihara, Plasma Phys. Contr. Fusion **45**, 1549 (2003).

[19]D. N. Hill, J. Nucl. Mater. **241**, 182 (1997).